



EXPERIMENTAL INVESTIGATIONS ON TIG WELDING OF ALUMINIUM 6351 ALLOY

* Venkata Ramana M¹, Sriram P S N² and Jayanthi A³

Department of Automobile Engineering, VNR Vignana Jyothi Institute of Engineering and Technology, Hyderabad, 500090, India.

ABSTRACT

The welding parameters play vital role in joining the work pieces and properties of the weld joints. The aim of the present work is to improve the mechanical properties of AA 6351 Aluminum alloy with pulsed Tungsten Inert Gas (TIG) welding process. Taguchi robust design methodology is applied to optimize the welding parameters to improve the mechanical properties. Analysis of Mean (AoM) is carried out to find the optimum process parameters. Analysis of Variance (ANOVA) is performed to analyze the influence of process parameters on mechanical properties. Microstructures of all the weld joints are analyzed.

Key words: Aluminium alloy, Tungsten Inert Gas, Tensile test, Micro hardness test, Microstructure,

Taguchi's methodology.

1. Introduction

Aluminum alloy has excellent performance in aerospace, marine, automobile, defense, nuclear, food processing and other applications. TIG welding is an arc welding process that uses a non-consumable tungsten electrode to produce weld. The weld area is protected from atmosphere by an inert shielding gas (argon or helium) and a filler metal is normally used. An electric arc is then created between the tungsten electrode and the work piece using a constant-current welding power supply that produces energy and conducted across the arc through a column of highly ionized gas and metal vapors. The electric arc can produce temperatures upto 20,000°C and this heat can be focused to melt and join two different parts of material. The current carrying capacity of each size of electrode depends on whether it is connected to negative or positive terminal of DC power source. The power source required to maintain the TIG arc has a dropping or constant current characteristic which provides an essentially constant current output when the arc length is varied over several millimeters. Hence, the natural variations in the arc length which occur in manual welding have little effect on welding current. TIG welding process has advantages over other arc welding process such as arrow concentrated arc, able to weld ferrous and non-ferrous metals, does not use flux or leave any slag and no spatter and fumes during TIG welding. The TIG welding process is best suited for metal plate of

thickness around 5 – 6 mm. The influence of pulsed welding parameters like base current, peak current, frequency, welding speed on mechanical properties such as yield strength, ultimate tensile strength and hardness of AA 5456 Aluminum alloy welds has been studied [1]. Effects of pulsed current on the of welding characteristics using TIG are studied on 304 stainless steel. More hardness is found in the HAZ zone of all the weldments due to grain refinement. Higher tensile strength is found in the non-pulsed current weldments. It was observed that ultimate tensile strength and yield strength of non-pulsed current are more than the parent metal and pulsed current weldments [2]. Multi response optimization such as ultimate tensile strength and yield strength and impact toughness is carried out on TIG weldments of Incoloy 800HT using grey relational analysis for quality weld joints. It is observed that the welding current highly influenced followed by welding speed and voltage on weldments [3]. An experimental investigation has been carried out on microstructure and corrosion resistance of weld butt joints of AA 2024-T3. Conventional tungsten inert gas and friction stir welding (FSW) processes have been considered. Micro hardness measurements pointed out that general decay of mechanical properties of TIG joints due to high temperatures experienced by work material [4].

The influence of input welding parameters on output variables like toughness, hardness, microstructure and macrostructure is carried on weldments of Aluminium alloy 5083. The combination of welding current 200A and shielding gas flow rate 15

*Corresponding Author - E- mail: mandalavenki@gmail.com

l/min are found to be better result [5]. A 12 mm thick double side square butt joint on 2.25Cr-1Mo (P22) steel plates using A-TIG welding process with in-house developed activated fluxes were done. Microstructure and mechanical properties of the weld joint were characterized. In the welded condition toughness was found to be 133 J. After PWHT, the toughness of weld was increased to 177 J due to dissolution and coarsening of existing precipitates [6].

Mechanical properties of the weldments of AA6351 during the TIG welding with non-pulsed and pulsed current at different frequencies were investigated. Welding was performed with current 70-74 A, arc travel speed of 700-760 mm/min and pulse frequency 3 and 7 Hz. From the experimental results it was concluded that the tensile strength and yield strength of the weldments is closer to base metal [7]. Understanding of different welding techniques and to find the best welding technique for steel was carried. It was found that TIG welded specimens can bear yield stress, higher load and tensile strength as compared to MIG welded specimens [8]. The high helium content gases are used for MIG welding of thicker materials, pure argon can be used for both MIG and TIG welding of Aluminum. Helium has a lower density than argon and higher flow rates are used when welding with helium, this can improve the productivity [9]. Experimental trials were performed to identify the working range of welding parameters like welding current, welding speed and gas flow rate after specimen preparation [10]. From the literature review, it is found that welding of Aluminum is a big challenge by conventional arc welding process. In this work TIG welding of Aluminum 6351 is investigated with varying welding parameters.

2. Experimental details

The experimental details and procedure is discussed below in detail as:

2.1 Base material

Commercial Aluminum (AA 6351) plate of thickness 5 mm is selected as work piece material for the present work and is tested for chemical composition. The chemical composition of the raw material is given in Table 1.

2.2 Filler material

Filler rods are used nearly in all applications of TIG, the major exception being the welding of thin materials. Filler metals are available with different diameters and are made of a variety of materials. Filler material adds the appropriate alloying elements to the welded materials that they lose during the welding process. Also it adds strength to the weld joint. In the

present work filler rod chosen is Aluminum 4351 alloy and it is generally preferred in TIG welding of Aluminum grades of 6XXX.

2.3 Welding process parameters

Welding is performed by varying input parameters like welding current, gas flow rate and root gap. The input welding parameters used in this work are given in Table 2. The voltage is varied from 12 to 15 V, the distance of tip from weld center is maintained 3 mm constant and the power source used is DCSP.

2.4 Electrodes for TIG welding

The electrode used in TIG is made of tungsten or a tungsten alloy, because tungsten has the highest melting temperature among pure metals at 3,422 °C. As a result, the electrode is not consumed during welding, though some erosion (called burn-off) can occur. The diameter of the electrode can vary between 0.5 and 6.4 millimeters and their length can range from 75 to 610 millimeters. In the present work Tungsten electrodes containing zirconium oxide is used. Presence of zirconium in tungsten electrode increases the current carrying capacity with improved arc stability and electrode life.

2.5 Shielding gas

Shielding gases are necessary in TIG to protect the welding area from atmospheric gases such as Nitrogen and Oxygen, which can cause fusion defects and weld metal embrittlement if they come in contact with the electrode and the arc or the welding metal. The gas also transfers heat from the tungsten electrode to the metal and it helps start and maintain a stable arc. The selection of a shielding gas depends on several factors, including the type of material being welded, joint design and desired final weld appearance.

Table 1. Chemical composition of Aluminum 6351

Material	Aluminum
Si	0.74
Fe	0.254
Cu	0.083
Mn	0.52
Mg	0.74
Zn	0.015
Ni	0.032
Cr	0.018
Ti	0.023
Al	Remaining

Argon is the most commonly used shielding gas for TIG, since it helps in preventing defects due to a varying arc length. Another common shielding gas is Helium, it is most often used to increase the weld penetration in a joint, to increase the welding speed and to weld metals with high heat conductivity such as

Copper and Aluminum. In the present work, Argon gas is used as shielding gas.

Table 2. Working range of process parameters

S.No.	Process parameter	Units	Lower level (1)	Middle level (2)	Higher level (3)
1	Set current (A)	Amps	170	180	190
2	Argon gas flow Rate (B)	lit/min	10	12	14
3	Root gap (C)	mm	1.5	2	2.5
4	Pulse frequency (D)	Hz	0	2	4

3. Experimental procedure

3.1 Methodology

In this work, Taguchi robust design methodology is used to obtain the optimum conditions of the experimental data. Statistical software Minitab is also used to obtain results for AoM and ANOVA using Design of Experiments. The output parameters chosen are Ultimate Tensile Strength(UTS) and Hardness.

3.2 Sample preparation for TIG welding

Aluminium plate are cut with dimension of 100 mm x 50 x 5 mm with the help of jig saw. Cutting is followed by grinding to smooth the burrs. These Aluminium pieces are then subjected to bevel grinding at an angle of 45° so that there should be a better root penetration. Bevel grinded samples are subjected to pickling process (cleaning process using 70% water and 30% nitric acid) to remove any external foreign particles.

3.3 TIG welding

After sample preparation, Aluminium plates are fixed side by side on the working table with flexible clamps and welding is done to get a butt joint. The end of the electrode was prepared by reducing the tip diameter to 2/3 of the original diameter by grinding and then striking an arc on a scrap material piece. This creates a ball on the end of the electrode. Experiments are performed by varying the input parameters as given in Table 3.

4. Results and discussions

The following sections discuss the results of the present experimental work. After performing the welding, tensile test specimen of dimensions shown in Figure 1 is cut from each sample. Tensile test is

performed on universal tensile testing machine (Instron-600) with maximum load capacity of 600 kN. These experimental results are given in Table 3.

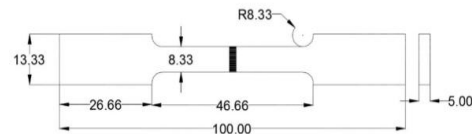


Fig. 1 Dimensions of tensile test specimen

4.1 Optimization of process parameters for tensile strength

Analysis of Mean is applied to find out the optimum process parameters. Means of S/N ratios is plotted and shown in Figure 2. The optimum process parameters to maximize the tensile strength are set current at level 3 (190 A), gas flow rate at level 1 (10 lit/min), root gap at level 1 (1.5 mm) and number of pulses at level 3 (4 pulses). Thus, the optimum conditions obtained are A3-B1-C1-D3 combination. A confirmation experiment is performed with the optimum process parameters. The tensile strength under these conditions is 176.34 MPa and corresponding S/N ratio is 44.97 dB. The prediction model is developed using S/N ratio of optimum process parameters. The S/N ratio under these conditions is 44.94 dB. The S/N ratio value of verification test is within the limits of the predicted value and the objective is fulfilled. Hence, these suggested optimum conditions can be adopted.

4.2 Optimization of process parameters for micro hardness

All the nine test specimens are subjected to micro hardness testing. Hardness is measured for each specimen at three different zones i.e. weld zone, heat affected zone (HAZ) and at base material. This test enables us to understand the change in mechanical property of the weldment throughout its length. In the present work, hardness at weldzone is considered for optimization process. Analysis of Mean is applied to find out the optimum process parameters. Means of S/N ratios is plotted and shown in Figure 3. The optimum process parameters to maximize the microhardness are set current at level 3 (190 A), gas flow rate at level 3 (14 lit/min), root gap at level 3 (2.5 mm) and number of pulses at level 3 (4 pulses). Thus, the optimum conditions obtained are A3-B3-C3-D3 combination. A confirmation experiment is performed with the optimum process parameters. The micro hardness under these conditions is 51.2 HV and corresponding S/N ratio is 34.189 dB. The prediction model is developed using S/N ratio of optimum process parameters. The S/N ratio under these conditions is 34.185 dB. The S/N ratio

value of verification test is within the limits of the predicted value and the objective is fulfilled.

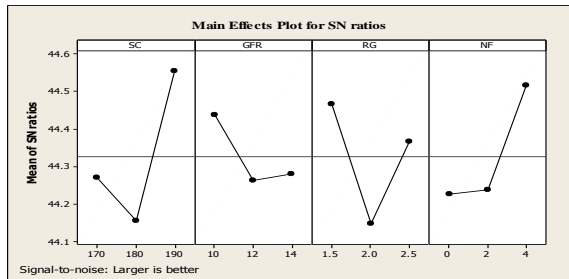
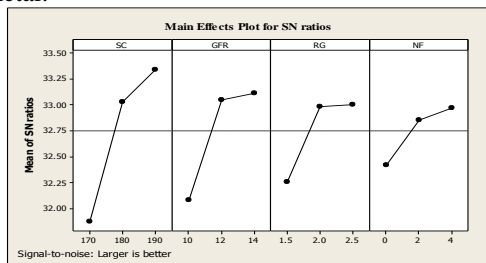


Fig. 2 Main effect plot for tensile strength

Hence, these suggested optimum conditions can be adopted. From the results of hardness test it was found that the Hardness of weld zone change with the distance from weld center due to change of microstructure.

It is found that the hardness of the weld zone is lower than that of hardness of the HAZ and the hardness of the HAZ is less than that of hardness of the base metal.



4.3 Analysis of variance

Fig. 3 Main effect plot for micro hardness

Analysis of variance is carried out to find the influence of process parameters on for tensile strength and hardness. These results are given in Table 4 and Table 5 respectively. The tabulated F-ratio ($F_{(0.05,2,9)}$) is 4.26. It was found that F- ratio calculated greater than the F- ratio tabulated. This concludes that the factors selected are significantly influencing the process. The set current is influencing more on tensile strength followed by number of pulses, root gap and gas flow rate. Similarly set current is influencing more on microhardness followed by gas flow rate, root gap and number of pulses.

Table 4. Analysis of variance for tensile strength

FACTOR	SS	DOF	MSS	F-RATIO	SS'	P (%)
SC	186.31	2	93.155	163.64	186.31	40.28
GFR	37.92	2	18.961	33.31	37.92	8.20
RG	115.75	2	57.876	101.67	115.75	25.03
NF	117.34	2	58.675	103.07	117.34	25.37
ERROR	5.123	9	0.569	-	5.123	1.12
TOTAL	462.45	17	-	-	-	-

Table 5. Analysis of variance for hardness

FACTOR	SS	DOF	M.S.S	F-RATIO	SS'	P (%)
SC	157.72	2	79.36	196.22	79.36	52.24
GFR	84.70	2	42.35	104.71	84.70	27.88
RG	41.40	2	20.70	51.18	41.40	13.63
NF	15.33	2	7.667	18.96	15.33	5.04
ERROR	3.640	9	0.404	-	3.640	1.21
TOTAL	303.78	17	-	-	-	100

Table 3. Observation table

Experiment No.	Levels of input parameters				Ultimate Tensile Strength (MPa)				Micro hardness (HV)			
	A	B	C	D	Trail 1	Trail 2	Average	S/N Ratio	Trail 1	Trail 2	Average	S/N Ratio
1	1	1	1	1	165.986	166.715	166.3505	44.42042	33.7	32.4	33.05	30.37839
2	1	2	2	2	157.918	156.847	157.3825	43.93898	41.4	43.1	42.25	32.51126
3	1	3	3	3	166.666	167.251	166.9585	44.45213	43.4	43.1	43.25	32.71957
4	2	1	2	3	164.073	163.145	163.609	44.27604	44	43.5	43.75	32.81914
5	2	2	3	1	158.278	159.867	159.0725	44.03158	45.8	46.3	46.05	33.26421
6	2	3	1	2	161.897	160.897	161.397	44.15778	44.2	45.3	44.75	33.01389
7	3	1	3	2	170.715	169.547	170.131	44.61552	44.6	45.1	44.85	33.03484
8	3	2	1	3	174.912	173.475	174.1935	44.82042	46.4	46.8	46.6	33.36748
9	3	3	2	1	163.038	162.397	162.7175	44.22863	48.3	47.6	47.95	33.61508



Fig. 4 Micro Structure of Base material at weld zone

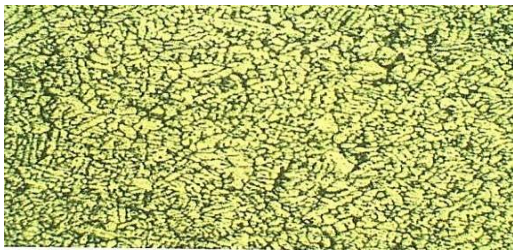


Fig. 5 Micro Structure of Sample 1 at weld zone



Fig. 6 Micro Structure Analysis of Sample 1 at HAZ

4.4 Microstructure study

Microstructure characterization studies are conducted on polished and chemically etched samples to study the metallurgical characterization of grains and secondary phases. The microstructure of base metal is shown in Fig. 4. The experimental condition 1 resulted with fine equiaxed grains at weld zone as shown in Fig. 5 and uniform grains with small precipitates can be observed in the HAZ as shown in Fig.6.

The experimental condition 2 shows that interdendritic network of aluminium with Mg precipitates in the weld zone is shown in Fig. 7. Uniform grains with precipitates are formed in the HAZ as shown in Fig. 8. The experimental condition 3 is resulted with fine equiaxed grains at weld zone as shown in Fig. 9 and fine grain structure with very small precipitates in the HAZ can be seen in Fig. 10. Considering the experimental condition 4, interdendritic network of Aluminum with Magnesium precipitates can

be observed in Fig. 11 and fine grain structure with small precipitates in the HAZ can be seen in Fig. 12. A fine equiaxed grains at weld zone is observed under experimental conditions 5 and 6 as shown in Fig. 13 and 15. Fine grain structures with very small precipitates are observed in the HAZ as shown in Fig. 14 and 16. The experimental condition 7 shows that interdendritic network of aluminium with Mg precipitates in the weld zone is shown in Fig. 17. Uniform small grains with small precipitates are formed in the HAZ as shown in Fig. 18. The experimental condition 8 shows that interdendritic large network of aluminium with very small Mg precipitates in the weld zone as shown in Fig. 19. Uniform grains with very small precipitates are formed in the HAZ as shown in Fig. 20. The experimental condition 9 shows that interdendritic network of aluminium with small Mg precipitates in the weld zone is shown in Fig. 21. Small grains with very small precipitates are formed in the HAZ as shown in Fig. 22.



Fig. 7 Micro Structure of Sample 2 at weld zone

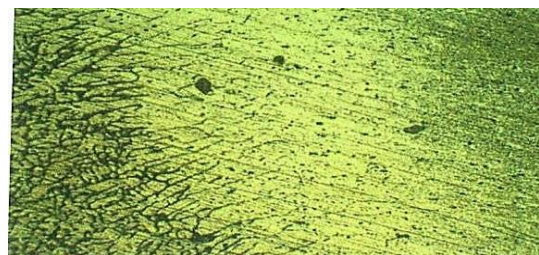


Fig. 8 Micro Structure Analysis of Sample 2 at HAZ



Fig. 9 Micro Structure of Sample 3 at weld zone

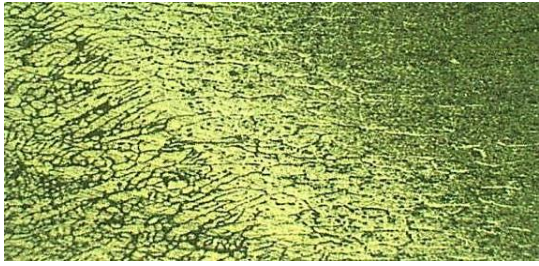


Fig. 10 Micro Structure Analysis of Sample 3 at HAZ

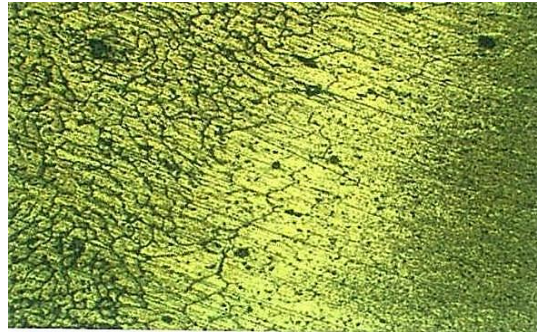


Fig. 14 Micro Structure Analysis of Sample 5 at HAZ

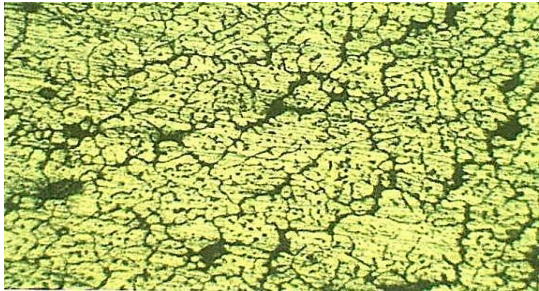


Fig. 11 Micro Structure of Sample 4 at weld

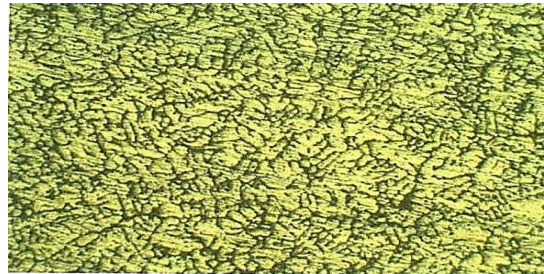


Fig. 15 Micro Structure of Sample 6 at weld zone

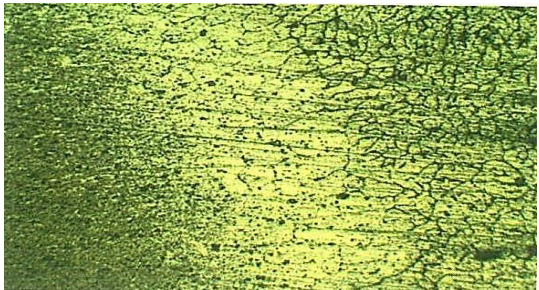


Fig. 12 Micro Structure Analysis of Sample 4 at HAZ

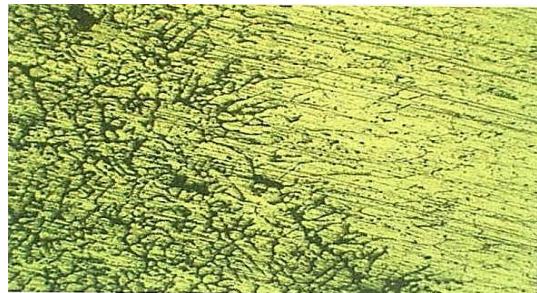


Fig. 16 Micro Structure Analysis of Sample 6 at HAZ

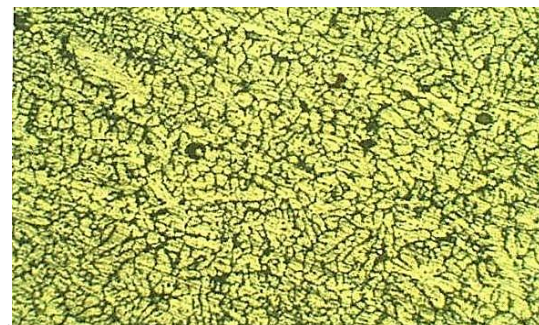


Fig. 13 Micro Structure of Sample 5 at weld zone

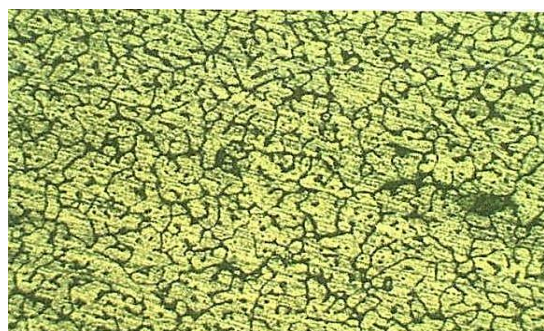


Fig. 17 Micro Structure of Sample 7 at weld zone

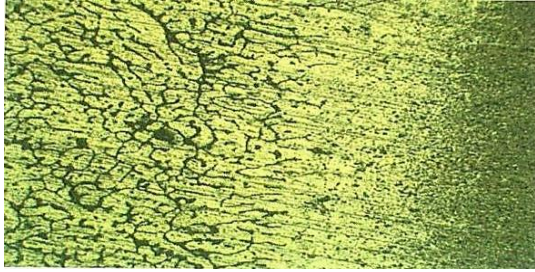


Fig.18 Micro Structure Analysis of Sample 7 at HAZ



Fig. 22 Micro Structure Analysis of Sample 9 at HAZ

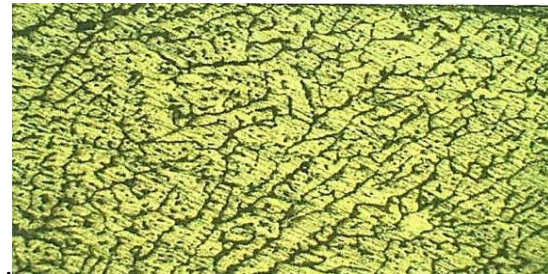


Fig. 19 Micro Structure of Sample 8 at weld zone

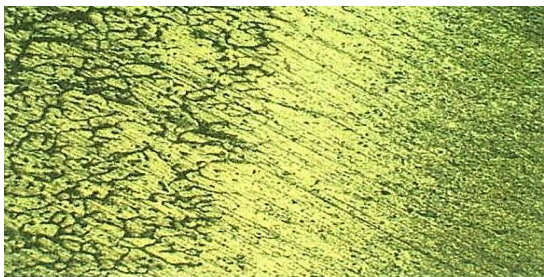


Fig. 20 Micro Structure Analysis of Sample 8 at HAZ

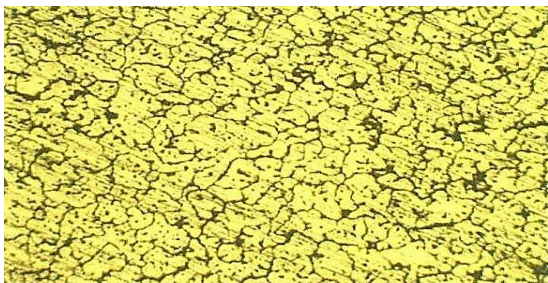


Fig. 21 Micro Structure of Sample 9 at weld zone

5. Conclusion

Experiments are conducted using design of experiments to optimize the welding parameter for maximization of tensile strength and hardness. The optimum conditions obtained to maximize the tensile strength are set current at 190 A, gas flow rate at 10 lit/min, root gap at 1.5 mm and number of pulses at 4. The optimum conditions obtained to maximize the hardness are set current at 190 A, gas flow rate at 14 lit/min, root gap at 2.5 mm and number of pulses at 4. The set current is contributed (40.28 %) more to enhance the tensile strength of weldment, followed by number of pulses, root gap and gas flow rate. The set current is contributed (52.24 %) more to enhance the hardness of weldment, followed by gas flow rate, root gap and number of pulses. The Hardness of heat affected zone is decreased and the weld zone hardness is found to be lower than hardness of heat affected zone which is due to weld penetration, type of filler rod and area of weld pool. Micro structure of heat affected zone revealed that fine intermetallic particles and uniform distribution of grains, which indicates better strength and hardness of the weldment. Micro structure of weld zone has shown that fine grains of intermetallic particles and uniform or non uniform elongated grain flow pattern.

References

1. Kumar A and Sundarrajan S (2009), "Optimization of pulsed TIG welding process parameters on mechanical properties of AA 5456 Aluminum alloy weldments", *Materials and Design*, Vol.30, 1288–1297.
2. Raveendra A and Kumar B R (2013), "Experimental study on Pulsed and Non-Pulsed Current TIG Welding of Stainless Steel Sheet (SS304)", *International Journal of Innovative Research in science in Science, Engineering and Technology*, Vol. 2(6), 2337-2344.
3. Arun Kumar Srirangan and Sathiya Paulraj (2015), "Multi-response optimization of process parameters for TIG welding of Incoloy 800HT by Taguchi grey relational analysis", *Engineering Science and Technology, an International Journal*.
4. Squillace A De Fenzo A Giorleo G and Bellucci F (2004), "A comparison between FSW and TIG welding techniques: modifications of microstructure and pitting corrosion resistance in AA 2024-T3 butt joints", *Journal of Materials Processing Technology*. Vol.152, 97–105.

5. Narayanan Arun Mathew Cijo Yeldo Vinod and Joseph Joby (2013), "Influence of Gas Tungsten Arc Welding Parameters in Aluminium 5083 Alloy", *International Journal of Engineering Science and Innovative Technology (IJESIT)*, Vol. 2(5), 269 -277.
6. Arivazhangan B and Vasudevan M (2015), "Studies on A-TIG welding of 2.25Cr-1Mo (P22) steel", *Journal of Manufacturing Processes*, Vol.18, 55-59.
7. Indira Rani M and Marpu R N (2012), "Effect of Pulsed Current TIG Welding Parameters on Mechanical Properties of J-Joint Strength of AA6351", *The International Journal of Engineering and Science*, Vol. 1(1),1-5.
8. Kazi Javed Zaid Syed Mohd Talha Syed Yasir Mukri and Akib Dakhwe (2015), "A Review on Various Welding Techniques", *International Journal of Modern Engineering Research*, Vol.5 (2), 22-28.
9. Prakash Jyoti Tewari S P and Srivastava Kumar Bipin (2011), "Shielding Gas for Welding of Aluminium Alloys by TIG/MIG Welding – A Review", *International Journal of Modern Engineering Research*, Vol. 1(2), 690 - 699.
10. Singh Lakshman Shah Vinay and Singh Naveen (2013), "Influence of TIG Welding Parameters On Weld Characteristics of 5083 Aluminium Alloy", *International Journal of Engineering Science and Innovative Technology*, Vol. 2(5), 462-468.